Realization of Thousand-Second Improved Confinement Plasma with Super I-Mode in Tokamak EAST

Yuntao Song[1], Xiaolan Zou[2*], Xianzu Gong[1*], Alain Becoulet[3], Richard Buttery[4] , Paul Bonoli[5], Tuong Hoang[2], Xiaoming Zhong[6], Adi Liu[6], Erzhong Li[1], Qing Zang[1], Jinping Qian[1], Haiqing Liu[1], Liang Wang[1], Liqing Xu[1], Ling Zhang[1], Guoqiang Li[1], Andrea Garofalo[4], Tom Osborne[4], Tony Leonard[4], Seung Gyou Baek[5], Greg Wallace[5], Shouxin Wang[1], Yuqi Chu[1], Tao Zhang[1], Yanmin Duan[1], Hui Lian[7], Xuexi Zhang[1], Yifei Jin[1], Rui Ding[1], Bo Lyu[1], Bin Zhang[1], Xiaojie Wang[1], Bojiang Ding[1], Miaohui Li[1], Xinjun Zhang[1], Chengming Qing[1], Weibin Xi[1], Jian Zhang[1], Liansheng Huang[1], Damao Yao[1], Yanlan Hu[1], Guizhong Zuo[1], Qinping Yuan[1], Zhiwei Zhou[1], Mao Wang[1], Handong Xu[1], Yahong Xie[1], Zhengchu Wang[1], Guosheng Xu[1], Jiansheng Hu[1], Kun Lu[1], Fukun Liu[1], Baonian Wan[1], Jiangang Li[1], and EAST Team

1*Institute of Plasma Physics, Chinese Academy of Sciences, Hefei 230031, China*
2*CEA, IRFM, F-13108 St Paul Les Durance, France*
3 *ITER Organization, Route de Vinon sur Verdon, 13115 St Paul Lez Durance, France*
4*General Atomics, PO Box 85608, San Diego, CA 92186-5608, USA*
5*Plasma Science and Fusion Center, Massachusetts Institute of Technology, Cambridge, MA, USA*
6*University of Science and Technology of China, Hefei, Anhui 230026, China*
7*University of California Los Angeles, Los Angeles, California 90095, USA*

**Email:* xiao-lan.zou@cea.fr, xz_gong@ipp.ac.cn

Abstract: Mastering nuclear fusion, which is an abundant, safe and environmentally competitive energy, is a great challenge for humanity. Tokamak represents one of the most promising paths towards controlled fusion. Obtaining high performance, steady-state and long-pulse plasma regime remains a critical issue. Recently, a big breakthrough in steady state operation was made on the Advanced Experimental Superconducting Tokamak (EAST). A stationary plasma with a world-record pulse length of 1056 s was obtained, where the density and the divertor peak heat flux were well controlled, with no core impurity accumulation. A new high-confinement and self-organising regime (Super I-mode = I-mode + e-ITB) is discovered and demonstrated. These achievements contribute to the integration of fusion plasma technology and physics, which is essential to operate next-step devices.

I. Introduction

With increasing global energy demand, our current energy sources, mainly fossil fuel reserves, must be substantially substituted with alternative nonfossil ones. Potential candidates include renewable and nuclear fission and fusion sources. Nuclear fusion, which powers the Sun, is the least developed of the three but is advantageous in terms of safety (only small quantities of nuclear waste with a short life generated) and environmental friendliness (no carbon dioxide production), offering a virtually inexhaustible energy source. Fusion research has concentrated primarily on high peak performance, with considerable progress made toward the generation of fusion energy, namely in TFTR (*1*) and JET (*2*). However, to ensure the feasibility of fusion reactors, the plasma performance must be sustained for long durations. This is often limited by the capacity of the machine and its subsystems and the plasma scenarios. Continuous operation of fusion reactors requires superconducting magnets, heating systems with a long-pulse capability, cooled plasma facing-components (PFCs) with the ability to handle injected power and ultimately the fusion power, and diagnostics and real-time feedback control algorithms for controlling the plasma.

Nearly all current magnetic confinement fusion devices rely on superconducting coil technology, including EAST (*3*), JT60-SA (Japan), KSTAR (Korea), SST1 (India), WEST (France), W7X (Germany), as well as the major next-step tokamaks: International Thermonuclear Experimental Reactor (ITER) (*4*) and China Fusion Engineering Test Reactor (CFETR) (5).

EAST is a medium-sized fully superconducting tokamak with actively cooled metallic PFCs; applying the same concept as ITER and CFETR; it has ITER-like magnetic configurations: major radius R = 1.85 m, minor radius a = 0.45 m, plasma current Ip = 1 MA, and toroidal field B_T = 3.5 T. Its mission is to address key technological and physics issues of long-pulse operation to support the design of reactor-grade machines. It is equipped with a total power of heating and current drive of 32 MW, including neutral beam injection heating (NBI) of 8 MW and radio frequency (RF) power of 24MW: i) Lower Hybrid Current Drive (LHCD) of 10MW (4MW at 2.45GHz, 6MW at 4.6GHz); ii) Electron cyclotron resonance frequency heating (ECRH) of 2MW at 140GHz; Ion cyclotron resonance frequency heating (ICRH) of 12MW at 27 MHz - 80 MHz. EAST's ITER-like tungsten (W) divertor has a power handling capability of ~10 MW m^{-2} for addressing plasma–wall interaction physics. Additionally, approximately 80 advanced diagnostics have been developed and implemented on EAST. These diagnostics allow the dynamics of plasma profiles, instabilities, and plasma–wall interactions to be measured during long-pulse operations. Therefore, EAST is a suitable platform to integrate technology and physics related to the long-duration operation of fusion plasmas (*3*). In particular, EAST, especially its divertor, can provide an ideal plasma–wall equilibrium to study the physics of plasma–wall interactions for next-step devices.

ITER (*6*) and CFETR are designed for steady-state operation with a duration of up to 1000 s. Previously, discharges lasting over 6 min have been achieved in Tore Supra (*4-7*), HT-7 (*8*) and EAST (*9*). In 2021, EAST reached a milestone, achieving plasma that could operate for a duration exceeding 1000 s and with injected/extracted energy of 2 GJ. This demonstrates the reliability of the machine and its subsystems (cryogenic, superconducting magnets, heating systems, and diagnostics) for long-pulse operation.

Heat and particle fluxes in the divertor target plates were actively controlled during the discharge for over 1056 s. A new physical phenomenon was also discovered. Plasma regime, called Super I-mode, was characterised by the coexistence of an electron internal transport barrier (e-ITB) at the plasma centre and an improved energy confinement mode (I-mode) at the plasma edge, leading to a large improved energy confinement. Discharges lasting from a few

hundred seconds to a thousand seconds showed an energy confinement much higher than that of the low-confinement plasma (L-mode), and comparable to the high-confinement mode (H-mode), which is envisaged as the basic operating mode of ITER.

II. Experiments

To access long-duration plasmas, experiments have been performed in a double-null magnetic configuration mainly using LHCD and ECRH at Ip =300–400 kA, B_T = 2.75 T, R=1.91 m, and a=0.45 m. B_T was chosen to be 2.75 T to simultaneously achieve on-axis ECRH deposition and optimised LHCD power absorption at 4.6 GHz. The line-averaged electron density $\bar{n}_e$ was approximately 2×10^{19} m^{-3}. The operational conditions were carefully tuned shot-by-shot, keeping the main parameters, such as heating powers, plasma density, plasma current, and plasma shape, the same.

Both particles and heat exhaust related to plasma–wall interaction must be controlled to operate long pulses. Therefore, real-time feedback control was implemented on EAST using additional relevant techniques. The plasma position was switched up/down during discharge to avoid excessive heat flux on PFCs. A powder dropper was used to inject lithium to mitigate impurities and reduce recycling. This allows control of density and radiated power due to impurities. Note that low particle recycling is favourable for cryo-pumping, which does not suffer from saturation or release of particles back into the plasma when in a low recycling regime.

Repeated tests of the plasma control system were performed each day prior to the experiments to minimise the error due to the offset of integrators of magnetic measurements, which is essential for controlling both the position (zero shift) and shape of the plasmas. Thus, a stable gap (~4 cm) between the plasma and the wall was maintained in the double-null configuration, ensuring sufficient particle exhaust.

After repetitive discharges of hundreds of seconds, a discharge with a duration of 1056 s was achieved, as shown in Fig. 1. A total energy of 2 GJ was injected into the plasma, twice as much as the record previously held by Tore Supra and EAST. Plasma was operated at Ip=330 kA and $\bar{n}_e = 1.8\times10^{19}m^{-3}$; it was heated by a total RF power of 1.65 MW (1.1 MW of LHCD at 4.6 GHz, and 0.55 MW of ECRH). As shown in the figure, all the main plasma quantities are stationary during the entire discharge. The radiation power, with tungsten (W) as the major radiating species, is found to be very low (~150 kW). Note that the discharge is fully non-inductive, i.e., the plasma current is mainly driven by LHCD and a moderate bootstrap current (~37%).

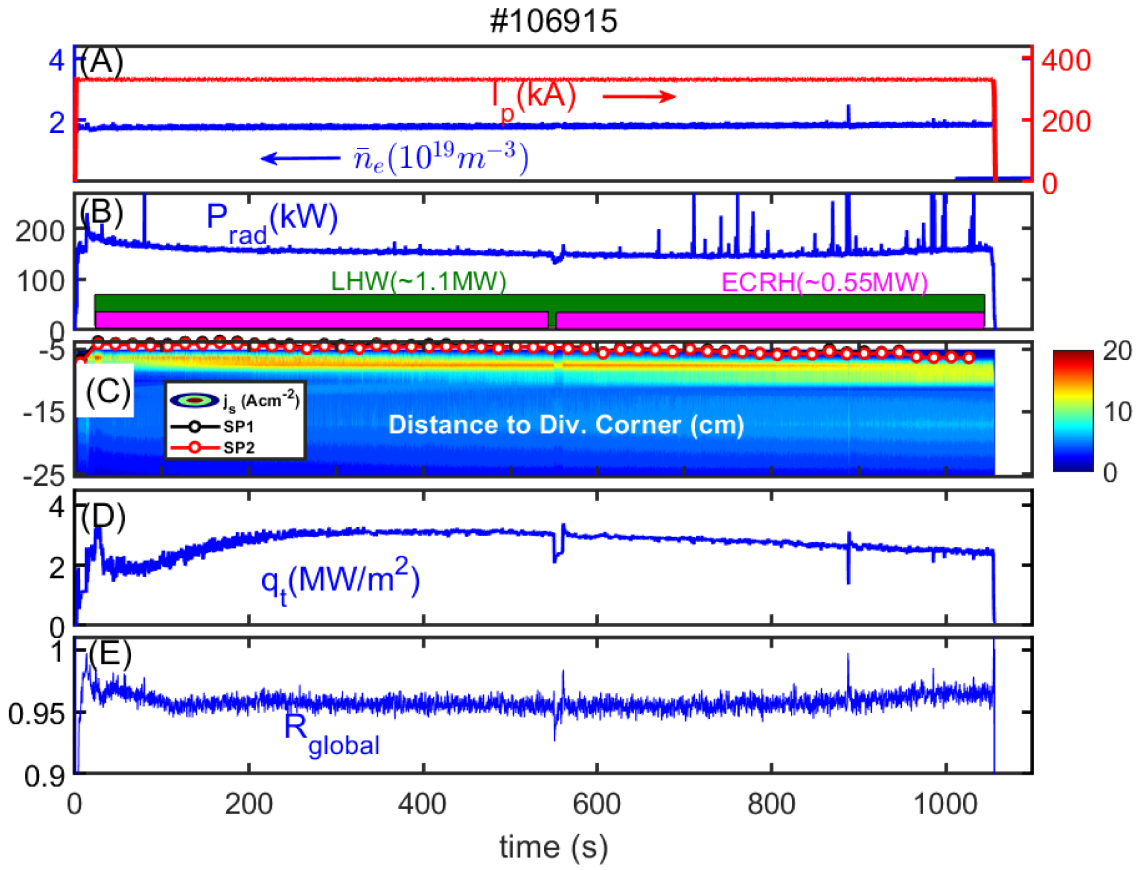

Fig. 1. Waveform of the thousand-second discharge #106915. (**A**) Plasma current I_p and line-averaged electron density $\bar{n}_e$. (**B**) LHCD, ECRH and radiated powers. (**C**) Contour of particle flux given by the ion saturation current j_s on the divertor target, with the strike points calculated from EFIT equilibrium shown in open circles (SP1 for outer strike point and SP2 for inner strike point). (**D**) Peak heat flux on the divertor target. (**E**) Global recycling coefficient.

III. Plasma–wall interactions

Plasma–wall interactions are not an operational issue in the long-pulse experiments discussed in this paper. At 1000 s, the particle flux on the divertor remained extremely stable, and the global recycling coefficient R_{global} was stationary at ~0.95, as shown in Fig. 1e. This is owing to the optimisation of the strike point position to realise better particle exhaust, along with the enhanced wall pumping using real-time wall conditioning by continuous lithium powder injection (1.3mg/s) from t=7s until the end of the discharge, which can effectively getter deuterium. The result suggests that the wall is not saturated at 1056 s. Thus, EAST becomes a platform for studying the physics of plasma–wall interactions under ideal conditions where plasma–wall equilibrium—on the time scale of tens of minutes is required.

Heat fluxes on PFCs and the divertor remained at moderate values. Steady-state peak heat flux on the divertor target plates was well controlled, remaining below 3 MW/m^2 (Fig. 1d), considerably lower than the power exhaust capability of the water-cooled tungsten divertor in EAST (10 MW/m^2).

Spectroscopic measurements indicate the low concentrations of light and/or heavy impurities, which is consistent with the low radiated power shown in Fig. 1b. W impurity is the dominant factor contributing to total radiation power loss. The concentration of W is considerably lower than that of a similar discharge observed in H-mode, as shown in Fig. 2. Such a low W concentration can be explained by the L-mode like particle transport, an insufficient W source observed in the absence of ELMs, and thanks to optimization of plasma current, RF heating power coupling and real-time Li powder injection. Moreover, the divertor electron temperature measured by Langmuir probes is 15-20 eV during the discharge, favouring a relative low W source which exhibits a strong dependence on the electron temperature at the target plates.

Note that W was not accumulated in the core over 1000 s. This behaviour is similar to that observed in WEST plasmas heated by RF powers, which is explained by the low torque driven by the RF waves *(10)*. Indeed, the increase of central W accumulation is due to the neoclassical convection increasing with toroidal rotation. Therefore, the result obtained is promising for low torque operation in the ITER.

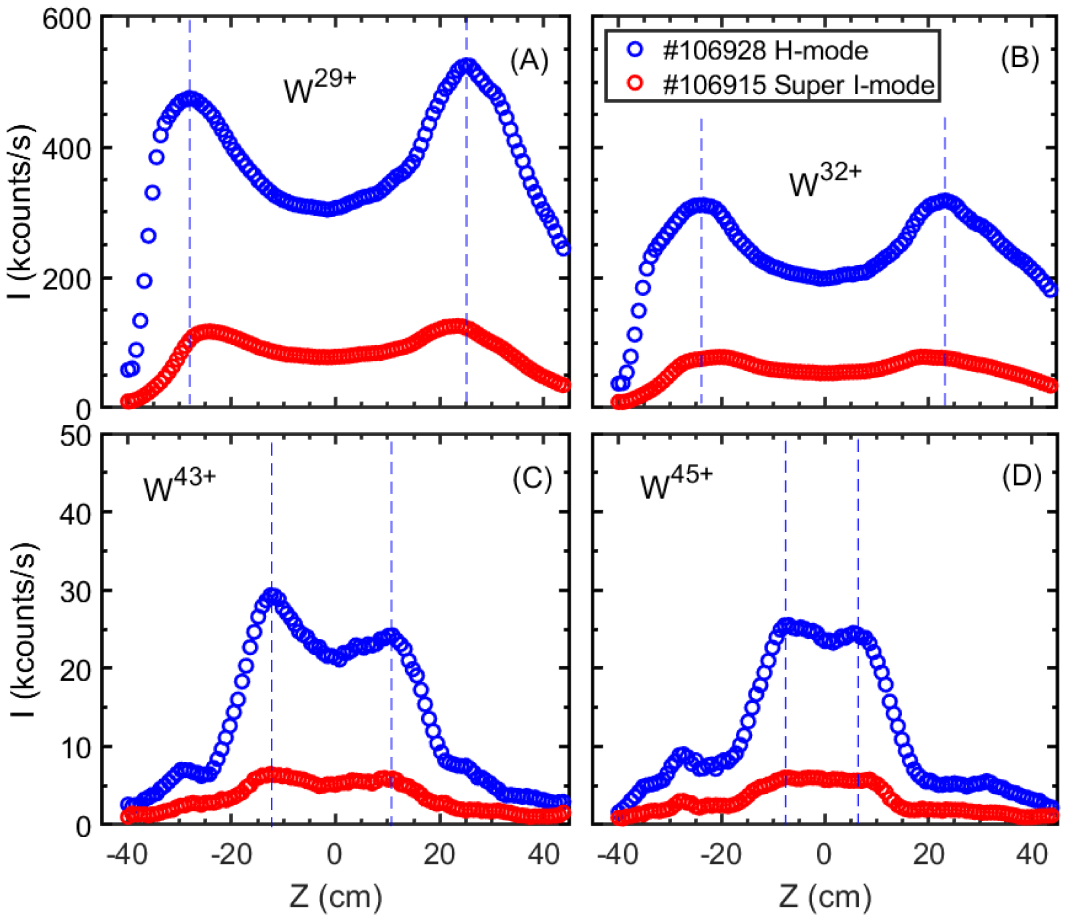

Fig. 2. Tungsten (W) impurity radiation. Line intensity profiles of W ions in discharge #106915, compared with discharges operated in L-mode and H-mode (#106928: I_p = 400 kA, 2 MW of LHCD, 1MW of ECRH). **(A)** $W29^+$, **(B)** $W32^+$, **(C)** $W43^+$, and **(D)** $W45^+$. (Vertical dashed lines indicate peak position of line intensities in H-mode)

IV. Super I-mode

H-mode *(11)*, characterised by the edge transport barriers of both density and temperature profiles, is considered as the baseline operation scenario for the ITER. Unacceptable heat flux to the divertor targets caused by large edge-localised-modes (ELMs) due to the relaxation of the edge transport barrier is still a crucial issue in fusion research *(12)*. For a fusion reactor, the ideal situation would be to have high energy confinement and low particle confinement. I-mode meets this criterion better than H-mode. Indeed, I-mode is a plasma regime with energy confinement similar to that in H-mode, and edge particle transport comparable to that in L-mode. I-mode was initially discovered on Alcator C-Mod *(13)* and ASDEX *(14)* and is characterised by an extremely steep edge temperature pedestal with the absence of the edge density pedestal and ELMs. The I-mode operation regime has several advantages over H-mode, such as preventing metallic impurity central accumulation, facilitating fusion product ash removal, and sustaining quiet stationary temperature pedestal, and thus, is more suitable for application in the fusion reactor. A regime with double transport barrier combining ITB and I-mode, named as Super I-mode, was discovered in discharges with durations ranging from 14–1055 s.

In the EAST tokamak, stationary I-mode is identified by the weakly coherent mode (WCM) *(15)* and edge temperature ring oscillation (ETRO) *(16)*. The ETRO, radially localised at the pedestal with an azimuthally symmetric structure, results from the ion/electron turbulence periodic transition. The WCM corresponds to electron turbulence, leading to L-mode-like particle transport. The stationarity of I-mode is due to the plasma self-organisation by coupling electron temperature gradient oscillation, turbulence transition, and heat transport modulation *(16)*.

The energy confinement of discharge #106915 matches that of the one predicted in H-mode. Indeed, the confinement time τ_E is higher than the value predicted by the H-mode scaling law $\tau^H_{Scaling}$ *(17)* by 20%, the energy confinement enhancement factor $H_{98} = \tau_E/\tau^H_{Scaling}$ =1.2 (Fig. 3A). Stored energy is 90 kJ, corresponding to the normalised plasma pressure $\beta_p = \langle p\rangle/\left(B_p{}^2/2\mu_0\right)$ ~ 1.5, which is the ratio of the plasma pressure to the magnetic pressure, characterizing the plasma performance. Here, $\langle p\rangle$ is the mean plasma pressure, and B_p the poloidal magnetic field. The central electron temperature $T_e(0)$ exceeds 6 keV and remains almost constant throughout the whole discharge (Fig. 3B). The central ion temperature $T_i(0)$ is about 0.7 keV.

I-mode is identified in discharge #106915 by detecting the WCM and ETRO, which are obtained from the power frequency spectrum of the time derivative of the density fluctuation phase dϕ/dt, measured using a Doppler reflectometer at the normalised radius ρ=0.91, and lasts for almost the whole discharge, as shown in Fig. 3C and Fig. 3D. The brief anomaly observed in WCM and ETRO spectra around t=570 s is due to a sudden and brief shutdown of the gyrotron (see Fig. 1B). The WCM frequency is in the range of 30–100 kHz and the ETRO frequency is approximately 14 kHz.

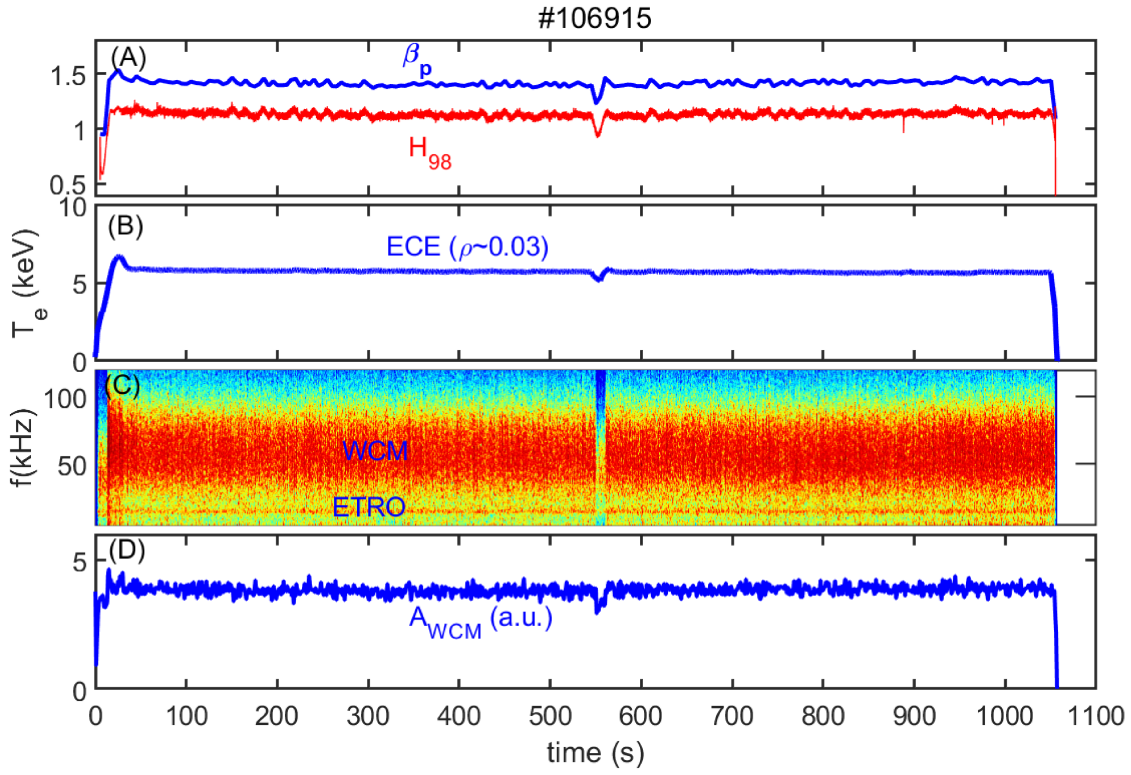

Fig. 3. I-mode identification. (A) Energy confinement enhancement factor H_{98} and the normalised plasma pressure β_p. **(B)** Electron temperature T_e measured at $\rho = 0.03$ by ECE. Note that the central ECE measurement is less affected by the suprathermal electron generated by LHCD, in addition is calibrated with Thomson scattering. **(C)** Frequency spectrogram of the time derivative of the density fluctuation phase $d\phi/dt$ measured using a Doppler reflectometer at $\rho = 0.91$, showing WCM (30-100 kHz) and ETRO (14 kHz). **(D)** Amplitude of WCM.

High confinement is related to evident improvements in both core and edge plasma. Fig. 4A and Fig.4B display in red the radial profiles of the electron temperature and density of the discharge #106915, respectively. Then these profiles are compared to that of L-mode (#106870, in blue) and H-mode (#107832, in green). An electron internal transport barrier (e-ITB) is observed at the plasma centre in the discharge #106915 as the H-mode, leading to a peaked central electron temperature. Simultaneously, an electron temperature pedestal is observed in this discharge at the plasma edge, similar to that in H-mode, as shown in Fig. 4C. However, in the absence of the pedestal, the edge density profile is extremely similar to that in L-mode, as show in Fig. 4D.

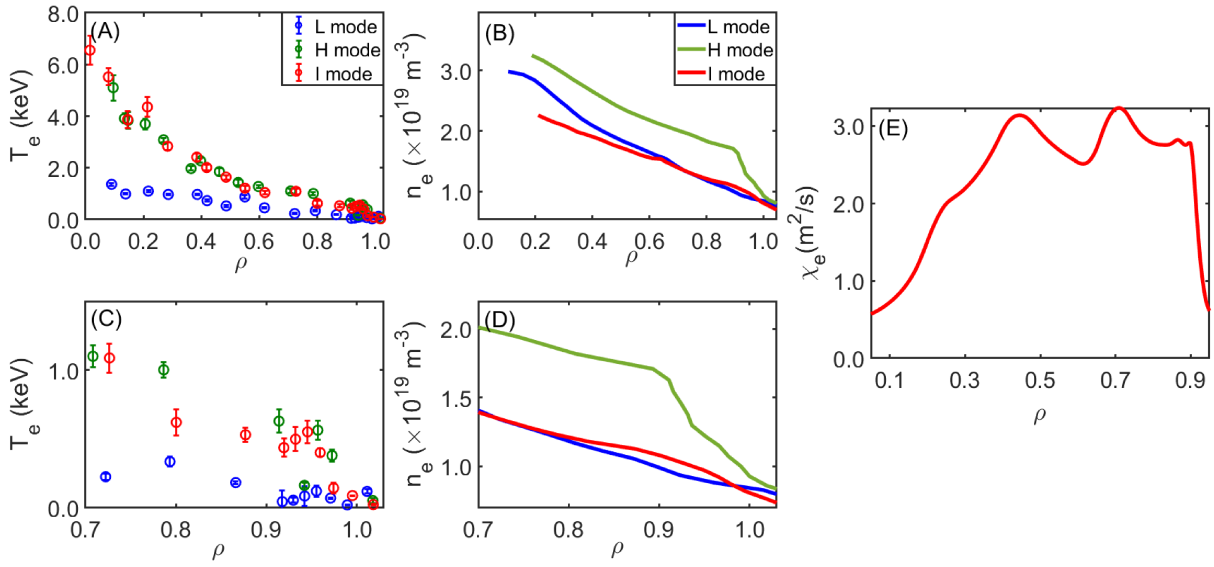

Fig. 4. Electron temperature and density profiles for transport analysis. The temperature and density radial profiles of Super I-mode (discharge #106915, in red) are compared to H-mode (discharges #107832, in green) and L-mode (discharge #106870, in blue). **(A)** Electron temperature profiles from the Thomson scattering diagnostic, showing evident ITB for super I-mode and H-mode. **(B)** Electron density profile from the reflectometer. **(C)** Zoomed view of the electron temperature profile at the edge for better differentiating the pedestal of super I-mode from L-mode. **(D)** Zoomed view of the electron density profile at the edge, showing similar edge density profile for super I-mode and L-mode. (**E**) Electron thermal conductivity in discharge #106915, deduced from the power balance analysis.

In discharge #106915, the electron temperature profile was found to be strongly peaked in ρ~0.4, exhibiting good correlation with the e-ITB location. The election thermal conductivity, obtained via a power balance analysis, decreases significantly to the neoclassical value at ρ = 0–0.4,

and ρ = 0.9–1.0, as shown in Fig. 4E, confirming is the presence of an edge transport barrier (I-mode) and a core transport barrier (ITB).

The magnetohydrodynamic activities (MHD) are continuously present in the plasma centre throughout this long pulse discharge (Fig. 5B). Fig. 5A displays the safety factor q profile measured using a POlarimeter-INTerferometer (POINT) in I-mode. A flat central q profile was identified by POINT to clamp the central q at values close to unity. Figs. 5C, Fig. 5D and Fig. 5E display the zoomed view (t =17.8s - 19s) of the MHD intensity, the normalized electron temperature gradient R/L_{Te} ($L_{Te}=(\nabla T_e/T_e)^{-1}$) and the turbulence intensity, respectively. It has been found that these latter three signals are modulated at the same frequency, indicating a strong interaction between MHD, turbulence and heat transport. The core e-ITB is identical to that observed in long pulse H-mode discharges as shown in Fig. 4. The physical mechanism for maintaining this e-ITB has been elucidated in （*18*） as follows. The electron-temperature-gradient-driven-mode (ETG) is excited when R/L_{Te} is above a threshold ($R/L_{Te} > 8$). Then, an intrinsic current is generated in the counter-current direction by ETG turbulence due to the divergence of the residual flux of the current, flattening the q profile at the centre and weakening the central magnetic shear, which causes turbulence reduction at the plasma centre. Finally, the MHD mode is periodically destabilised by the high electron temperature gradient in a low magnetic shear regime, serving as a sink to release the turbulence free energy, which causes a modulation of turbulence and turbulence-driven current. This self-regulation system serves as the automatic controller, which dynamically forces the electron temperature gradient in a proper region to sustain the kinetic equilibrium. Thus, a small amplitude oscillatory electron temperature profile around the critical temperature gradient triggering ETG is achieved, forming a quasi-stable and robust ITB.

.

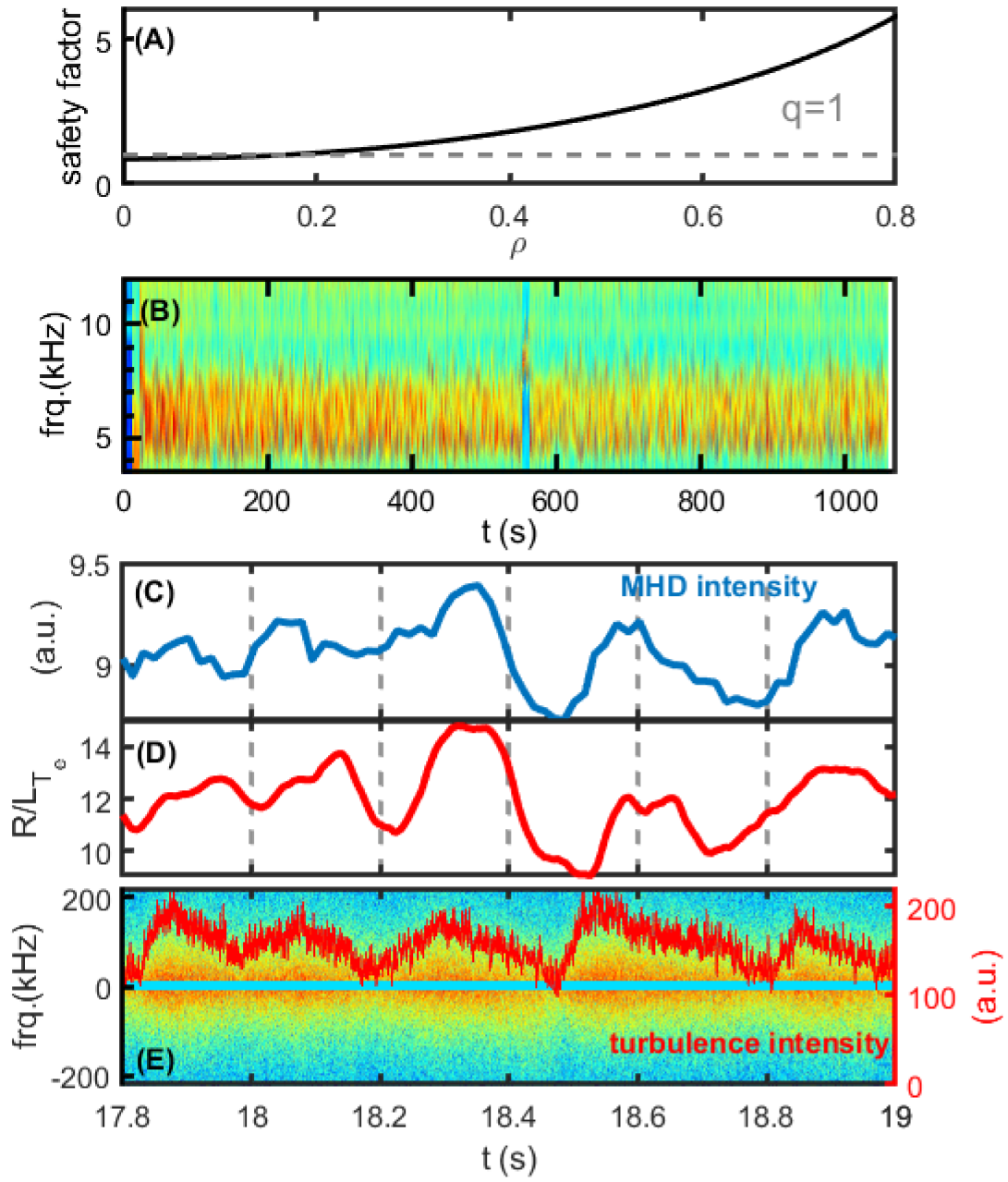

Fig. 5. Interaction between MHD, turbulence and electron heat transport for sustaining stationary ITB. (A) Safety factor q reconstructed using a POlarimeter-INTerferometer (POINT) system. **(B)** MHD frequency spectrum measured in the plasma core using SXR diagnostic, the MHD frequency is in the range of 4-8 kHz. **(C)** Zoomed view of MHD intensity at t = [17.8 19] s. **(D)** Normalized electron temperature gradient R/L_{Te} at t = [17.8 19] s. **(E)** Turbulence frequency spectrogram and intensity at t = [17.8 19] s.

Fig. 6 represents the energy confinement enhancement factor H_{98} as a function of the pulse length for Super I-mode (solid red square), standard I-mode (red square), H-mode (blue triangle), L-mode with ITB (violet circle), and standard L-mode without ITB (black diamond). Super I-mode has an energy confinement similar to that of H-mode, but with a pulse length considerably longer than that of H-mode. Further, compared with standard I-mode, Super I-

mode exhibits better energy confinement with a 50% higher H-factor. It should be noted that the present Super I-mode was obtained in the case of a very high electron temperature and a lower ion temperature. Super I-mode experiments on EAST will be extended towards the case of high ion temperature.

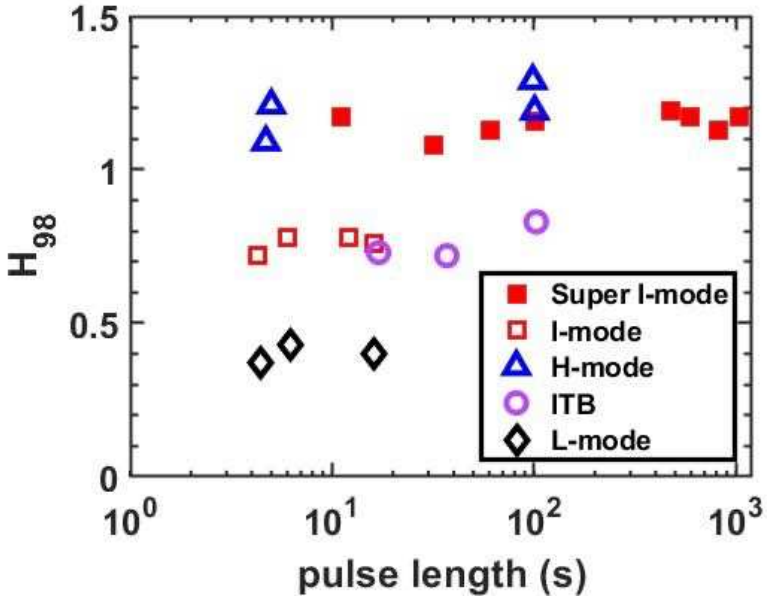

Fig. 6. Comparison for the energy confinement enhancement factor H_{98} and the plasma duration. Various plasma regimes obtained in EAST are compared: Super I-mode (solid red square), standard I-mode (red square), H-mode (blue triangle), L-mode with ITB (violet circle), and L-mode without ITB (black diamond).

V. Conclusions

The Institute of Plasma Physics, Chinese Academy of Sciences, has recently achieved progress regarding fusion reactors. A stationary plasma was successfully maintained for over 1056 s in the fully superconducting tokamak EAST. The machine and its subsystems (cryogenic, magnets, heating systems, diagnostic, etc.) were extremely reliable and operated safely owing to the integration of real-time controls and careful prior preparation.

Technology and fusion plasma physics were integrated. This achievement is mandatory to operate next-step devices, such as ITERs and CFETRs.

In addition to the operational aspect, a self-organising, highly steady with quiet pedestal, robust plasma regime was discovered, called Super I-mode. In this regime, I-mode co-exists with an electron internal transport barrier, leading to an enhancement of energy confinement with H_{98} ~1.2. Such a regime has advantages with respect to the integration of the plasma–wall interaction and high plasma performance on long time scales. The heat load on PFCs is moderate due to the absence of ELMs; further, ITB is maintained owing to plasma self-organisation without external control techniques for plasma stability. Therefore, Super I-mode exhibits potential for application in ITERs and CFETRs.

Acknowledgments

Dr Amanda Hubbard (MIT, USA) is acknowledged for fruitful discussions. This work is supported by the National Key R&D Program of China (Grant No. 2021YFE030203). This

work was also partly supported by China National Funds for Distinguished Young Scientists with No. 51525703 and National MCF Energy R&D Program (Grant No.2019YFE03040000).

References

1. M.G. Bell, et al., Overview of DT results from TFTR. *Nuclear Fusion* **35**, 1429 (1995).
2. J. Jacquinot, et al., Overview of ITER physics deuterium-tritium experiments in JET. *Nuclear Fusion* **39**, 235 (1999).
3. J. Li et al., Nature Physics 9, 817 (2013)
4. http://www.iter.org/
5. Y. Wan, et al., Overview of the present progress and activities on the CFETR. *Nuclear Fusion* **57**, 102009 (2017).
6. C. Gormezano, et al., Steady state operation. *Nuclear Fusion* **47**, S285 (2007).
7. D. van Houtte, et al., Recent fully non-inductive operation results in Tore Supra with 6 min, 1 GJ plasma discharges. *Nuclear Fusion* **44**, L11 (2004).
8. B. Wan, et al., Recent experiments in the EAST and HT-7 superconducting tokamaks. *Nuclear Fusion* **49**, 104011 (2009).
9. Y.T. Song, et al., The accomplishments and next-step plan of EAST in support of fusion. *IEEE Transactions on Plasma Science* **42**, 415–420 (2014). doi:10.1109/TPS.2014.2301159
10. J. Bucalossi, et al., Operating a full tungsten actively cooled tokamak: overview of WEST first phase of operation. *Nuclear Fusion* **62**, 042007 (2022).
11. F. Wagner, et al., Regime of improved confinement and high beta in neutral-beam-heated divertor discharges of the ASDEX tokamak. *Physical Review Letters* **49**, 1408 (1982).
12. A. Loarte, et al., ELM energy and particle losses and their extrapolation to burning plasma experiments. *Journal of Nuclear Materials* **313–316**, 962–966 (2003).
13. M. Greenwald, et al., H mode confinement in Alcator C-Mod. *Nuclear Fusion* **37**, 793 (1997).
14. F. Ryter, et al., H-mode power threshold and transition in ASDEX Upgrade. Plasma Physics and Controlled Fusion **40**, 725 (1998).
15. D.G. Whyte, et al., I-mode: an H-mode energy confinement regime with L-mode particle transport in Alcator C-Mod. Nuclear Fusion **50**, 105005 (2010).
16. A.D. Liu, et al., Experimental identification of edge temperature ring oscillation and alternating turbulence transitions near the pedestal top for sustaining stationary I-mode. Nuclear Fusion **60**, 126016 (2020).
17. ITER Physics Expert Groups on Confinement, Transport, Confinement Modeling and Database, ITER Physics Basis, Chapter 2: Plasma confinement and transport, Nuclear Fusion **39**, 2175 (1999).
18. E. Li, et al., Experimental evidence of intrinsic current generation by turbulence in stationary tokamak plasmas. Physical Review Letters **128**, 085003 (2022).